# Extreme tropical cyclone activities in the southern Pacific Ocean

Karl Hoarau, Ludovic Chalonge, Florence Pirard, Daniel Peyrusaubes

INTERNATIONAL JOURNAL OF CLIMATOLOGY
RMetS Royal Meteorological Society

# Extreme tropical cyclone activities in the southern Pacific Ocean

| | |
|---|---|
| Journal: | *International Journal of Climatology* |
| Manuscript ID | Draft |
| Wiley - Manuscript type: | Research Article |
| Date Submitted by the Author: | n/a |
| Complete List of Authors: | HOARAU, Karl; Cergy University, geography<br>Chalonge, Ludovic; University of Paris 1 Pantheon - Sorbonne, geography<br>PIRARD, Florence; Cergy University, Institute of Technology<br>Peyrusaubes, Daniel; University of Poitiers, geography |
| Keywords: | southern Pacific Ocean, categories 4 and 5 cyclones, global warming, decadal variations, El Niño event |
| | |

# Extreme tropical cyclone activities in the southern Pacific Ocean

Karl HOARAU

University of Cergy-Pontoise, 33 Boulevard du Port

95011 Cergy Cedex, FRANCE, phone 01 34 25 64 34, fax 01 34 25 64 42

KHoarau@aol.com

Ludovic CHALONGE

University of Paris 1 Pantheon - Sorbonne, 13 rue du Four

75006 Paris, FRANCE

Florence PIRARD

University of Cergy-Pontoise, Institute of Technology, 95-97 rue Valere Collas

95100 Argenteuil, FRANCE

Daniel PEYRUSAUBES

University of Poitiers, 5 rue Theodore Lefebvre

86073 Poitiers, FRANCE

**ABSTRACT:** This research concerning the South Pacific Ocean shows the ten-year and interannual variability of extreme cyclones (categories 4 and 5). The intensity of these cyclones has been reanalysed on the basis of GMS, GOES, and NOAA satellite images. In the period 1980 to 2016, 63 cyclones reached categories 4 and 5. During the decade 1980-89, the intensity of cyclones of at least 115 knots was underestimated: we found 19 such cyclones, as opposed to 6 in the Joint Typhoon Warning Center (JTWC) database. Between 1980 and 2016, the number of extreme cyclones did not show any tendency to increase. The 1983 season was the most active, with 6 cyclones of categories 4 and 5 that do not figure in the JTWC database for the South Pacific. El Niño episodes concurred with a much higher number of cyclones of at least 115 knots than La Niña episodes. More than half of the category 5 (at least 140 knots) cyclones were observed during El Niño years. While the ocean temperature is not a negligible explanatory factor, tropospheric dynamics remain determinant. The South Pacific Ocean is the theatre of very intense cyclones, comparable to those in the western or eastern North Pacific. Thus, by reanalysing satellite images, an intensity of 170 knots was attributed to cyclone Hina (March 1985), which was the strongest in the southern hemisphere since 1980.

**Key words:** southern Pacific Ocean; categories 4 and 5 cyclones; global warming; decadal variations; El Niño event.

## 1. Introduction

The South Pacific Ocean corresponds to the ocean basin located south of the equator and delimited in the west by the 135° East meridian. On average, every year, 10 tropical disturbances reach at least the tropical storm stage with 35 knots winds sustained for 1 minute (Diamond *et al.,* 2012; Walsh *et al.,* 2015). The present Joint Typhoon Warning Center's database (JTWC, 2015) shows that, on average, every year in the South Pacific Ocean, 1 tropical storm increased in intensity to a category 4 or 5 extreme cyclone (at least 115 knots) in the Saffir-Simpson classification (Simpson, 1974). In the debate on global warming and the variation in the number of category 4 and 5 extreme cyclones, research has produced very different results for the South Pacific Ocean. Webster *et al.* (2005) found that activity doubled between 1975-1989 and 1990-2004. Klotzbach (1986) indicates a moderate trend (+23%) towards an increase in the number of cyclones of at least 115 knots between 1986-1995 and 1996-2005 in the South Pacific. Kuleshov *et al.* (2010) have not mentioned any trend for the period 1982 to 2007. More recently, Klotzbach and Landsea (2015) have not revealed any trend between 1990 and 2014. These various research studies used existing archives concerning the intensity of cyclones of which the data had never been verified. On the basis of an automatic algorithm applied to satellite images, Kossin *et al.* (2007) estimated the intensity of cyclones on the worldwide scale between 1983 and 2005. Apart from the fact that this method reduces the accuracy of the estimated intensity compared to the Dvorak classic method (1984), Kossin *et al.* (2007) did not find any trend in the number of categories 4 and 5 cyclones for the South Pacific. In order to provide new light, this article deals with the original elements of the activity of category 4 and 5 extreme tropical cyclones in the South Pacific, based on the reanalysis of satellite images during the period 1980-2016.

## 2. Under-estimation of the intensity of cyclones in the decade 1980-1989.

The South Pacific Ocean was served for the period 1980-2016 by two geostationary satellites, GMS positioned at 140°E, and GOES-West at 135°W (Foley, 1995). While GMS satellites have always had a resolution of 4 km with infrared, GOES satellites had 8 km resolution in the 1980s. Also, these satellites could not always observe the real temperature of the warmest pixel in the eye of cyclones, considering the position of the cyclones or the small size of the eye. The temperature of the eye is an important parameter for estimating the intensity of cyclones from infrared images. Consequently, it was necessary to use images with 4 km resolution from polar orbiting satellites belonging to the National Oceanic and Atmospheric Administration (NOAA). While moving, these satellites can pass directly above cyclones and observe the warmest pixel in the eye. Indeed, the stage of intensity of a cyclone is determined by the Dvorak (1984) analysis, for which one needs to know the highest temperature in the eye and the temperature of the top of the clouds within a radius of 0.5 degree around the cyclone centre. The Dvorak Technique is based on cyclone operational procedures that are used to estimate the intensity by means of the maximum sustained wind over 1 minute. This Technique was published in 1984. Since forecasters need several months to learn about and experience this technique, an efficient application was effective in all the world's cyclone basins in the late 1980s (Knaff *et al.,* 2010). Furthermore, the assessment of the Dvorak Technique did not find any overestimation of the intensity of the strongest cyclones.

To illustrate the problem of the insufficient quality of databases concerning the intensity of cyclones pointed out by several authors (Landsea *et al*., 2006; Harper *et al*., 2008; Hoarau *et al*., 2012) including Kuleshov *et al*. (2010) on the subject of the South Pacific Ocean, we took the example of Isaac (22P), whose intensity is not known in the JTWC database (2015). This cyclone formed on 28 February 1982 east of the Samoa Islands and then moved towards the south-west (Figure 1).

**Figure 1**

On examining satellite images, marked cooling of the cloud tops was noted between the start and the middle of the day on 1 March (Figure 2), when Isaac's cloud configuration corresponded to 4.5 on the Dvorak (1984) scale, which goes up to 8.

**Figure 2**

The intensity is therefore estimated at 75 knots (Figure 3). On 2 March, the increase in intensity continues rapidly.

**Figure 3**

At 0600 UTC, a small eye forms in the central dense overcast (Figure 2). The eye widens and warms up to +18.4°C at 1500 UTC. The wide cloud belt of 0.5 degree includes tops with temperatures of -70°C to -77°C. The more the eye is warm and the more the cloud tops are cold, the greater is the intensity of the cyclone. At 1200 UTC and 1500 UTC, Isaac displayed satellite data of 7.0, which, in the Dvorak Technique, match with sustained winds of 140 knots. However, at 1800 UTC, satellite data figures drop to 6. This is why the maximum intensity of the cyclone is estimated at 130 knots (category 4) at 1500 UTC and 1800 UTC before its intensity starts decreasing (Figure 3). During a phase of rapid intensification, winds do not have time to adjust to the cloud configuration, and the same applies during a phase of rapid decrease (on 3 March from 0600 UTC): an increase or decrease of the strength of winds in the cyclone is delayed by a few hours in relation to satellite data.

Cyclone Isaac is not an isolated case. Comparison of our reanalysis with the JTWC database (2015) shows that the number of category 4 and 5 cyclones had been largely underestimated in the South Pacific during the decade 1980-89 (Figure 4): we found 19 cyclones that generated winds of at least 115 knots, as opposed to 6 found by JTWC. The ten-year distribution between 1980 and 2009 does not show a trend towards an increase in the number

of category 4 and 5 cyclones, even if activity in the present decade 2010-19 should be higher than activity in 2000-09.

**Figure 4**

When one considers the location of the maximum intensity of each of the 63 extreme cyclones in the South Pacific from 1980 to 2016, one finds that the geographical area concerned ranges from 10°S to 23°S and from 135°E to 145°W (figure 5). A total of 44 (70%) of the 63 category 4 and 5 cyclones, and 12 (66%) of the 18 category 5 cyclones (at least 140 knots) reached their maximum intensity west of the 180° meridian.

**Figure 5**

In the 1980s, a category 5 cyclone was observed at 147°W. It is the most intense cyclone listed in the south-eastern part of the Pacific Ocean. Most of the extreme cyclones reached their maximum between 12°S and 18°S. The four category 4 cyclones (115 to 135 knots) that reached their maximum intensity south of 20°S have occurred since 2010. This could confirm the poleward migration of the location of the maximum intensity of cyclones identified by Kossin *et al*. (2014). These different characteristics of the extreme cyclones activity in the South Pacific are greatly influenced by the interannual variations of oceanic and tropospheric conditions.

## 3. The indisputable role of the El Niño phenomenon

Marked interannual variability of the number of category 4 and 5 cyclones was found in the South Pacific (Figure 6). The maximum was 6 extreme cyclones during the summer of 1983, while none was observed 7 times between 1980 and 2016.

**Figure 6**

The 1983 season was under the influence of a strong El Niño episode (CPCM, 2016). None of the 6 extreme cyclones in 1983 is found in the JTWC database (2014) with an intensity of

more than 100 knots (Figure 7), while our reanalysis finds sustained winds over 1 minute ranging from 120 knots in the case of Tomasi (19P) on 30 March to 155 knots (7.5 on the Dvorak's scale) for Orama (13P) on 24 February.

**Figure 7**

Orama is the strongest cyclone in the eastern part of the basin. In the same year, Reva (17P) and Veena (21P) respectively reached 125 and 130 knots east of the 150°W meridian. While the two other strong El Niño episodes, in 1998 and 2016, did not concur with a high number of extreme cyclones (of which there were 2 in each of these years), the most moderate El Niños in 1992, 2003 and 2005 had more activity (Figure 6). In total, during the 9 El Niño episodes from 1980 to 2016, there were 28 category 4 and 5 cyclones, i.e., an average of 3.1 per year. This is a higher value than the average of 1.7 per year, if we count the 63 cyclones that occurred in 37 years. However, the 8 La Niña episodes produced 10 extreme cyclones, with an annual average of 1.25, a value comparable to that obtained on the basis of 25 extreme cyclones formed during the 20 other seasons in the South Pacific. Therefore, cyclones were of greater intensity during El Niño phases, and their location at the time of their maximum intensity was different from that of La Niña episodes or other seasons (Figure 8).

**Figure 8**

Among the 18 category 5 cyclones (at least 140 knots), 10 (55.55%) were observed during the 9 El Niño episodes, 3 (16.66%) during the 8 La Niña phases, and 5 (27.79%) during the 20 other seasons. During the El Niño episodes, category 4 and 5 cyclones reached their maximum between 160°E and 147°W, with a centre of gravity located around 15.5°S and 173°W. During La Niña phases, extreme cyclones reached their maximum at a position further west and further south, with a centre of gravity around 17.5°S and 160°E; no cyclone reached category 4 or 5 east of the 180° meridian. For the 20 other seasons, the centre of gravity was located at 16.5°S and 163°E. Concerning the differences of location between El

178 Niño and La Niña, our results for extreme cyclones concur with those found by several
179 authors who worked on the tropical storms and cyclones of the hurricane stage in the South
180 Pacific Ocean (Nicholls, 1979, 1984; Revel and Gouter, 1986; Basher and Zheng, 1995;
181 Chand and Walsh, 2011; Dowdy *et al.,* 2012; Chand *et al.,* 2013).
182 In addition, we compared the temperature of the ocean, firstly, between the 2 strongest El
183 Niño episodes, and secondly, between the 2 most marked La Niña phases (CPCM, 2016).
184 While the ocean temperature was higher in the South Pacific for El Niño in the summer of
185 2016 than in 1983 (Figure 9), the number of extreme cyclones was higher, and activity
186 extended further to the east in 1983.

187 **Figure 9**

188 Similarly, the ocean temperature was higher for La Niña in the summer of 2000 than in 1989
189 (Figure 10), and there were no extreme cyclones in 2000, as opposed to 2 in 1989. Therefore,
190 it is not only the higher ocean temperature in the eastern South Pacific during an El Niño
191 phase that explains the higher number of cyclones of at least 115 knots east of the 180°
192 meridian.

193 **Figure 10**

194 At the same time, the absence of category 4 and 5 cyclones east of the 180° meridian during
195 the La Niña episodes cannot be explained by the ocean temperature, which was at least 28°C
196 in February 1989 and 2000. Consequently, the conditions in the troposphere are determinant
197 in the South Pacific Ocean. During the El Niño, the cyclonic vorticity of low layers is stronger
198 in the monsoon trough that occupies a position between 170 degrees East and 140 degrees
199 West (Dowdy *et al.,* 2012; Chand *et al.,* 2013). Vertical wind shear reaches low figures to the
200 east of the 180° meridian, with winds at 200 hPa which have an eastward component (Basher
201 and Zheng, 1995; Ramsay *et al.*, 2008; Dowdy *et al.,* 2012; Chand *et al.,* 2013; Cheung *et al.*,
202 2014). Thus the eastward extension of favourable atmospheric conditions enables tropical

storms to develop and to become category 4 and 5 cyclones. During La Niña phases, the formation and intensification of cyclones take place in the western part of the ocean basin with unfavourable atmospheric conditions east of the 180° meridian.

## 4. The strongest cyclones in the South Pacific Ocean

It is always difficult to determine what are the most intense cyclones in a specific basin. Nott *et al.* (2014) put forward a pressure of 880 hPa for cyclone Mahina on the basis of the 9 metres storm tide that had hit Bathurst Bay in North-East Australia and a measurement of 914 hPa observed by a boat on 5 March 1899. Even if the authors consider Mahina to be the most intense cyclone ever recorded in the southern hemisphere, it is not possible to attribute an intensity to a cyclone for which there is no satellite data or wind data. In the JTWC database (2015), 2 cyclones were estimated at 155 knots in the South Pacific, that is, Zoe (06P) on 27 December 2002, and Monica (23P) on 23 April 2006. In real time, JTWC attributed an intensity of 155 knots to cyclone Winston (11P) on 20 February 2016. In a detailed study, Durden (2010) estimated Monica at 160 knots. Our reanalysis of satellite images of the South Pacific between 1980 and 2016 also enabled us to list the strongest cyclones. We identified cyclones that reached sustained winds of at least 155 knots, i.e., 7.5 on the Dvorak (1984) scale. In the satellite imagery, these cyclones are seen to have an eye with a temperature of more than +9°C, and with cloud tops colder than -75°C within a minimum radius of 0.5 degree around the centre. This was the case for Orama (Figure 7) and for the 3 cyclones already mentioned – Zoe, Monica and Winston – to which we added cyclones Anne (07P) on 10 January 1988 and Percy (20P) on 2 March 2005 (Figure 11), which have an intensity of 140 knots in the JTWC database (2015). During its phase of very rapid intensification, satellite data showed that Anne even reached 8 on the Dvorak (1984) scale, with clouds top temperature between -81°C and -90°C (Figure 11). However, this cloud

227 configuration did not remain long enough to allow this cyclone to be estimated at more than
228 155 knots.

229 **Figure 11**

230 In agreement with Durden (2010), our analysis attributes 160 knots to Monica. In fact, a
231 seventh cyclone exceeded 155 knots and, below, we study it in more detail, because it may be
232 considered as the most intense cyclone in the South Pacific.

233 This is cyclone Hina (30P), which was formed on 13 and 14 March 1985 north of the Vanuatu
234 Islands (Figure 12). This cyclone moved at more than 15 knots in the east-south-east
235 direction, then south-east, passing to the west of the Fiji Islands at the end of the day on 16
236 March.

237 **Figure 12**

238 From its very beginning, Hina intensified rapidly, increasing from 55 knots to 105 knots in 24
239 hours between 14 and 15 March at 0000 UTC (Figure 13). It is at that time that our analysis
240 starts to diverge from that of JTWC, which attributed a maximum intensity of 135 knots to
241 Hina on 16 March at 0600 UTC and 1200 UTC. For the same period, our estimation gives 170
242 knots, i.e., an intensity of 8 on the Dvorak (1984) scale.

243 **Figure 13**

244 Cyclone Hina had a cloud configuration of 140 knots on 15 March at 0300 UTC, 155 knots at
245 0600 UTC, and 170 knots on 16 January from 0300 UTC to 1200 UTC. The persistence of
246 satellite data at 155-170 knots for a period of more than 24 hours enabled sustained winds to
247 gradually adjust to the cloud scheme, explaining the exceptional intensity reached by cyclone
248 Hina. The satellite imagery shows that Hina had cold cloud tops from the beginning of the day
249 on 15 March (Figure 14). These cloud tops continued to cool while the eye was becoming
250 warmer.

251 **Figure 14**

Thus the closed cloud belt that included cloud tops colder than -81°C was extended to reach 0.5 degree at its narrowest part on 16 January from 0300 UTC, 0.6 degree at 0600 UTC, and 0.65 degree at 0900 UTC. At this time, certain cloud tops had a temperature of -92°C just around the eye. The perfectly circular eye with a diameter of 22 km had a temperature of +15°C on 15 January at 0330 UTC, +18°C at 1441 UTC, +21°C on 16 January at 0319 UTC, and still +20°C at 1500 UTC at the time when the cyclone started to weaken.

With an estimated intensity of 170 knots, Hina is probably the strongest cyclone in the southern hemisphere since the early 1980s. JTWC (2015) attributed winds of 150 knots to cyclone Agnielle (01S) on 21 November 1995 in the South Indian Ocean – an intensity similar to that attributed in real time to cyclone Fantala (19S) on 18 April 2016. However, there has still not been a reanalysis of cyclone intensities in this basin. Nevertheless, Hina could be one of the world's most intense cyclones since 1980. Only Patricia on 23 October 2015 in the North-East Pacific and Haiyan on 7 November 2013 in the North-West Pacific reached respectively 185 knots (Kimberlain *et al.*, 2016) and 170 knots (Lander *et al.*, 2014).

## 5. Conclusion

This study highlighted the particularities of category 4–5 extreme tropical cyclones in the southern Pacific Ocean over the period 1980-2016. The re-analysis of intensities using satellite images indicates that 63 extreme cyclones were formed over the last 37 years. The number of category 4 and 5 cyclones had been largely underestimated in the South Pacific during the decade 1980-89; we found 19 cyclones that generated winds of at least 115 knots, as opposed to 6 found by JTWC. This illustrates the problem of the insufficient quality of databases and why a reanalysis of cyclone intensities was needed. The decadal distribution did not reveal any trend towards an increase in the number of these cyclones. In fact, the number of cyclones at least at 115 knots has decreased from 19 in the 1980s to 14 in the

277 2000s. However, since 2010, the extreme cyclone activity is going up and the four category 4
278 cyclones (115 to 135 knots) that reached their maximum intensity south of 20°S have
279 occurred since that year. 70% of the 63 category 4 and 5 cyclones and 66% of the 18 category
280 5 cyclones (at least 140 knots) reached their maximum intensity west of the 180° meridian.

281 During the El Niño episodes, category 4 and 5 cyclones reached their maximum between
282 160°E and 147°W, with a centre of gravity located around 15.5°S and 173°W. During La
283 Niña phases, extreme cyclones reached their maximum at a position further west and further
284 south, with a centre of gravity around 17.5°S and 160°E; no cyclone reached category 4 or 5
285 east of the 180° meridian. For the 20 other seasons, the centre of gravity was located at 16.5°S
286 and 163°E. Cyclones were of greater intensity during El Niño phases. The 9 El Niño episodes
287 from 1980 to 2016 produced 28 category 4 and 5 cyclones, i.e., an average of 3.1 per year.
288 The 8 La Niña episodes generated 10 extreme cyclones, with an annual average of 1.25, a
289 value comparable to that obtained on the basis of 25 extreme cyclones formed during the 20
290 other seasons in the South Pacific.

291 While the ocean temperature was higher in the South Pacific for El Niño than for La Niña,
292 especially east of the 180° meridian, tropospheric dynamics remain determinant. During El
293 Niño events, the eastward extension of favourable atmospheric conditions enables tropical
294 storms to reach category 4 and 5 cyclones until 147°W. During La Niña phases, the
295 intensification of cyclones takes place in the western part of the ocean basin with
296 unfavourable atmospheric conditions east of the 180° meridian whereas the sea surface
297 temperature was at least at 28°C.

298 Even if the southern Pacific Ocean is not the more active cyclonic basin, seven extreme
299 cyclones have reached an intensity of at least 155 knots between 1980 and 2016. Orama, Hina
300 and Anne formed in the 1980's; Zoe, Percy and Monica reached their peak in the 2000's. And
301 Winston is the only cyclone at 155 knots for the period 2000-2016. Therefore, there is no

trend towards an increase of the strongest cyclones of the category 5. Moreover, our re-analysis shows that one cyclone, Hina in 1985, is estimated to have peaked at 170 knots. Hina is probably the more intense cyclone in the southern hemisphere since the early 1980s. Hina could be one of the world's most intense cyclones since the satellite era with typhoon Haiyan (November 2013) and hurricane Patricia (October 2015).

**Acknowledgements**

This work was funded by the University of Cergy-Pontoise, France. Grateful acknowledgements is made of the valuable comments by the reviewers.

**References**

Basher RE, Zheng X, 1995. Tropical cyclones in the southwest Pacific: Spatial patterns and relationships to Southern Oscillation and sea surface temperature. *Journal of Climate* **8**: 1249-1260.

Chand SS, Walsh KJE, 2011. Influence of ENSO on tropical cyclone intensity in the Fiji region. *Journal of Climate* **24**: 4096-4108.

Chand SS, McBride JL, Tory KJ, Wheeler MC, Walsh KJE, 2013. Impact of different ENSO regimes on southwest Pacific tropical cyclones. *Journal of Climate* **26**: 600-608.

Cheung KKW, Jiang N, Liu KS, Chan LTS, 2014. Interdecadal shift of intense tropical cyclone activity in the Southern Hemisphere. *International Journal of Climatology*, **34**, DOI: 10.1002/joc.4073.

Climate Prediction Center Maryland (CPCM), 2016. The Oceanic Nino Index.
http://www.cpc.noaa.gov/products/analysis_monitoring/ensostuff/ensoyears.shtml

323 Diamond HJ, Lorrey AM, Knapp KR, Levinson DH, 2012. Development of an enhanced
324 tropical cyclone tracks database for the southwest Pacific from 1840 to 2010. *International*
325 *Journal of Climatology* **32**: 2240-2250.

326 Dowdy AJ, Qi L, Jones D, 2012. Tropical Cyclone climatology of the South Pacific Ocean
327 and Its Relationship to El Niño-Southern Oscillation. *Journal of Climate,* **25**: 6108-6122.

328 Durden SL, 2010. Remote Sensing and Modeling of Cyclone Monica near Peak Intensity.
329 *Atmosphere,* **1**: 15-33.

330 Dvorak VF, 1984. Tropical cyclone intensity analysis using satellite data. *NOAA technical*
331 *Report NESDIS 11*: 47p.

332 Foley GR, 1995. Observations and analysis of tropical cyclones. Global Perspectives on
333 Tropical Cyclones. WMO/TD-No.693, Geneva: 1-20.

334 Harper BA, Stroud SA, McCormack M, West S, 2008. A review of historical tropical cyclone
335 intensity in northwestern Australia and implications for climate change trend analysis.
336 *Australian Meteorological Magazine,* **57**: 121-141.

337 Hoarau K, Bernard J, Chalonge L, 2012. Intense tropical cyclone activities in the northern
338 Indian Ocean. *International Journal of Climatology*, **31**: 1935-1945.

339 Joint Typhoon Warning Center (JTWC), 2015. The tropical cyclones best track data in the
340 southern hemisphere (1980-2015).
341 http://www.usno.navy.mil/NOOC/nmfc-ph/RSS/jtwc/best_tracks/shindex.php

342 Kimberlain TB, Blake ES, Cangialosi JP, 2016. Hurricane Patricia 20-24 October 2016
343 (EP202015). *National Hurricane Center Tropical Cyclone Report*. NOAA, 32p.

344 Klotzbach PJ, 2006. Trends in global tropical cyclone activity over the past twenty years
345 (1986-2005). Geophysical Research Letters, **33**, doi: 10.1029/2006GL025881.

346 Klotzbach PJ, Landsea CW, 2015. Extremely Intense Hurricanes: Revisiting Webster et al.
347 (2005) after 10 Years. *Journal of Climate* **28**: 7621-7629.

348 Knaff JA, Brown DP, Courtney J, Gallina JG, Beven JL, 2010. An evaluation of Dvorak
349 technique–based tropical cyclone intensity estimates. *Weather and Forecasting* **25**: 1362–
350 1379.

351 Kossin JP, Knapp KR, Vimont DJ, Murnane RJ, Harper BA, 2007. A globally consistent
352 reanalysis of hurricane variability and trends. Geophysical Research Letters **34**.
353 10.1029/2006GL028836.

354 Kossin JP, Emanuel KA, Vecchi GA, 2014. The poleward migration of the location of
355 tropical cyclone maximum intensity. *Nature,* **509**: 349-352.

356 Kuleshov Y, Fawcett R, Qi L, Trewin B, Jones D, McBride J, Ramsay H, 2010. Trends in
357 tropical cyclones in the South Indian Ocean and the South Pacific Ocean. *Journal of*
358 *Geophysical Research*, **115**, doi: 10.1029/2009JD012372.

359 Lander M, Guard C, Camargo SJ, 2014. State of the climate in 2013. *BAMS* **95**: 112-114.

360 Landsea CW, Harper BA, Hoarau K, Knaff JA, 2006. Can We Detect Trends in Extreme
361 Tropical Cyclones? Science, **313**: 452-454.

362 Nicholls N, 1984. The Southern Oscillation, sea surface temperature, and interannual
363 fluctuactions in Australian tropical cyclone activity. *Journal of Climatology* **4**: 661-670.

364 Nicholls N, 1979. A possible method for predicting seasonal tropical cyclone activity in the
365 Australian region. *Monthly Weather Review* **107**: 1221-1224.

366 Nott J, Green C, Townsend I, Callaghan J, 2014. The world record storm surge and the most
367 intense southern hemisphere tropical cyclone, new evidence and modeling. *Bulletin of*
368 *American Meteorological Society,* **95**: 757-765.

Ramsay HA, Leslie LM, Lamb PJ, Richman MB, Leplastrier M, 2008. Interannual Variability of Tropical Cyclones in the Australian Region: Role of Large-Scale Environment. *Journal of Climate* **21**: 1083-1103.

Revell CG, Goulter SW, 1986a. South Pacific tropical cyclones and the Southern Oscillation. *Monthly Weather Review* **114**: 1138-1145.

Simpson B, 1974. The Hurricane disaster potential scale. *Weatherwise*, **27**: 169-186.

Walsh KJE, McBride JL, Klotzbach PJ, Balachandran S, Camargo SJ, Holland G, Knutson TR, Kossin J, Lee TC, Sobel A, Sugi M, 2015. Tropical cyclones and climate change. *WIREs Clim Change 2015*. Doi: 10.1002/wcc.371.

Webster PJ, Holland GJ, Curry JA, Chang HR, 2005. Changes in tropical cyclone number, duration, and intensity in a warming environment. *Science,* **309**: 1844-1846.

**Figure caption**

Figure 1. Trajectory of tropical cyclone Isaac (February-March 1982). Source: Chart created from data of JTWC.

Figure 2. Satellite images (Basic Dvorak) of cyclone Isaac. Source: Images treated using raw data from NCDC and JMA.

Figure 3. Estimation of the intensity of cyclone Isaac using the Dvorak method. Source: Chart created from raw data provided by GMS and NOAA.

Figure 4. Number of extreme category 4-5 cyclones per decade (1980-2016). Source: Chart prepared using data from JTWC and from the re-analysis of cyclone intensities by the authors.

Figure 5. The location of the maximum intensity of extreme cyclones in the southern Pacific Ocean. Source: Chart created from the re-analysis of cyclone intensities by the authors.

Figure 6. Annual number of extreme Cat 4-5 cyclones (1980-2016) and the El Niño, La Niña events. Source: Chart prepared using data from CPCM (2016) and the re-analysis of cyclone intensities by the authors.

Figure 7. Satellite images (Basic Dvorak) of extreme cyclones during the 1983 season. Source: Images treated using raw data from NCDC.

Figure 8. The location of the maximum intensity of extreme cyclones during El Niño, La Niña and the other seasons. Source: Chart prepared using data from CPMC (2016) and the re-analysis of cyclone intensities by the authors.

Figure 9. The location of the maximum intensity of extreme cyclones and the sea surface temperature during the two strongest El Niño events. Source: Chart prepared using data from NOAA/ESRL and from the re-analysis of cyclone intensities by the authors.

Figure 10. The location of the maximum intensity of extreme cyclones and the sea surface temperature during the two strongest La Niña events. Source: Chart prepared using data from NOAA/ESRL and from the re-analysis of cyclone intensities by the authors.

Figure 11. Satellite images (Basic Dvorak) of five of the seven strongest cyclones in the southern Pacific Ocean. Source: Images treated using raw data from NCDC.

418 Figure 12. Trajectory of tropical cyclone Hina (March 1985). Source: Chart created from data
419 of JTWC.
420
421 Figure 13. Estimation of the intensity of cyclone Hina using the Dvorak method. Source:
422 Chart created from raw data provided by GMS, NOAA and JTWC.
423
424 Figure 14. Satellite images (Basic Dvorak) of cyclone Hina. Source: Images treated using raw
425 data from NCDC and JMA.

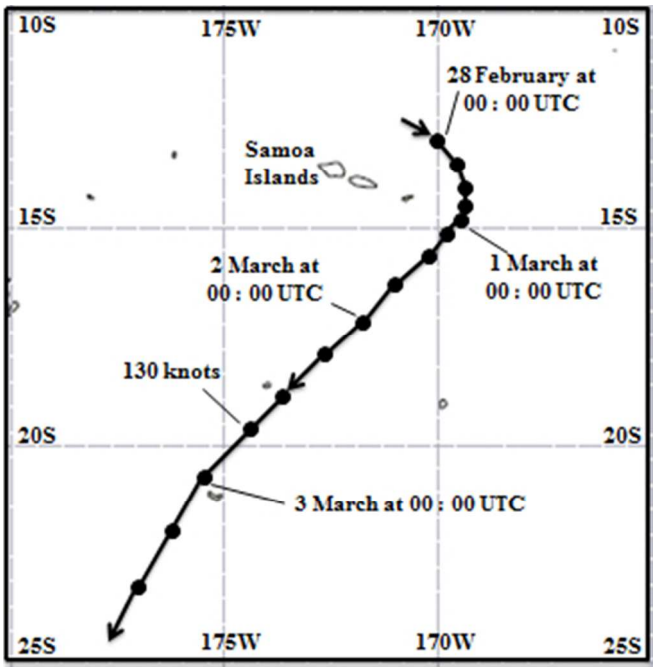


Figure 1. Trajectory of tropical cyclone Isaac (February-March 1982). Source: Chart created from data of JTWC.

114x116mm (72 x 72 DPI)

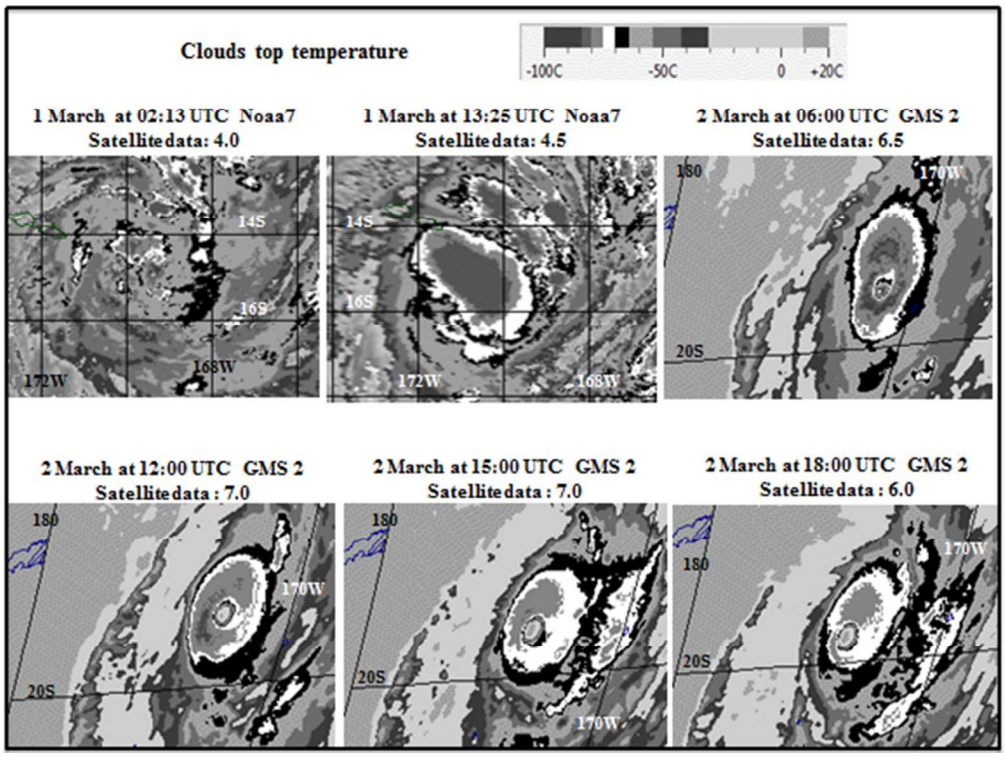


Figure 2. Satellite images (Basic Dvorak) of cyclone Isaac. Source: Images treated using raw data from NCDC and JMA.

203x152mm (72 x 72 DPI)

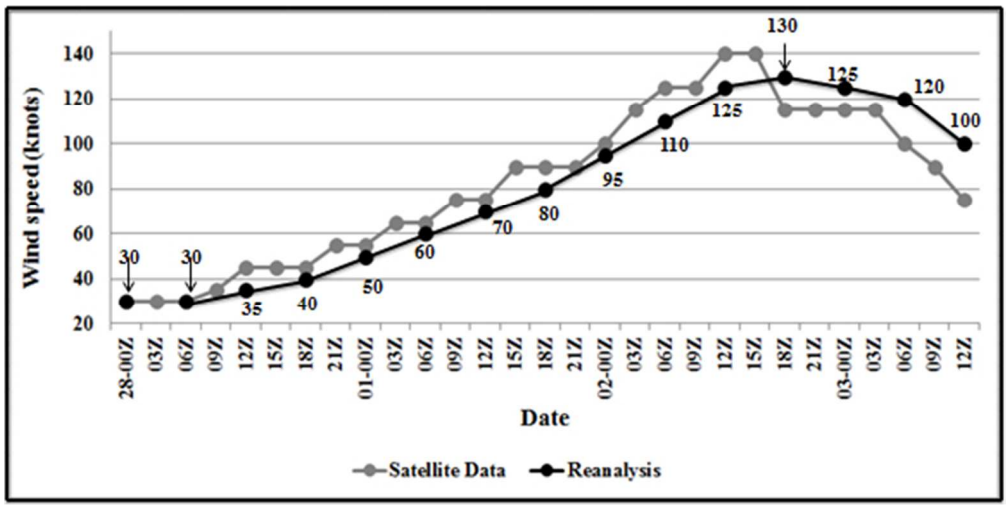


Figure 3. Estimation of the intensity of cyclone Isaac using the Dvorak method. Source: Chart created from raw data provided by GMS and NOAA.

204x101mm (72 x 72 DPI)

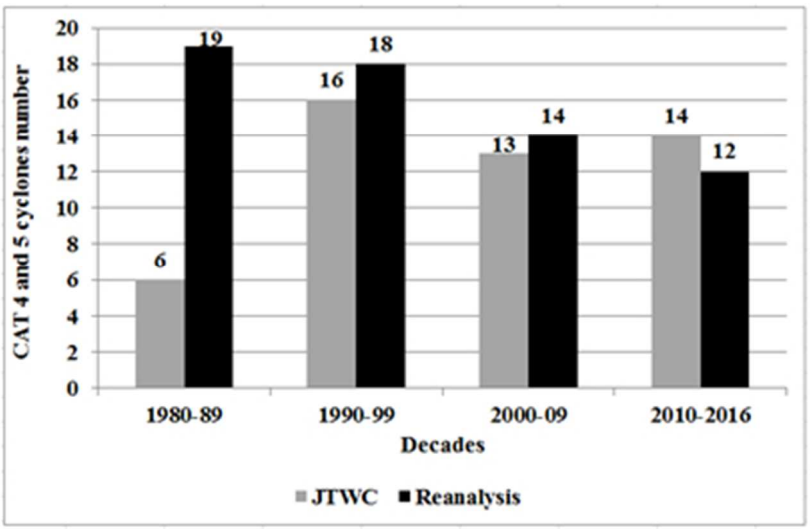


Figure 4. Number of extreme category 4-5 cyclones per decade (1980-2016). Source: Chart prepared using data from JTWC and from the re-analysis of cyclone intensities by the authors.

142x92mm (72 x 72 DPI)

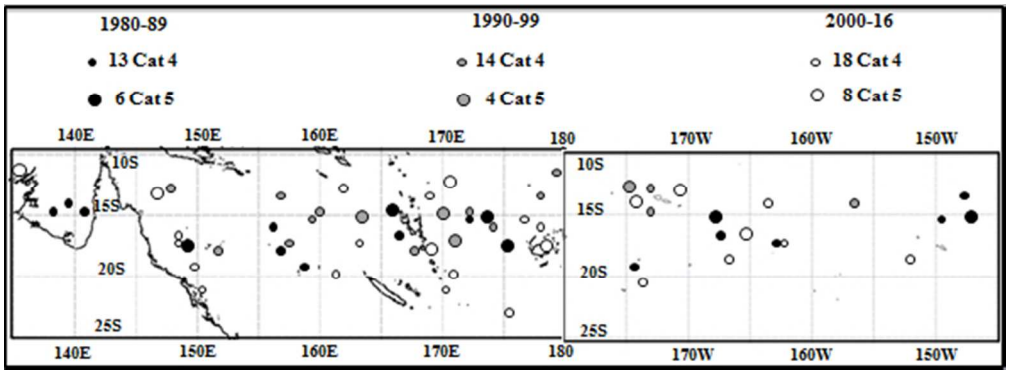


Figure 5. The location of the maximum intensity of extreme cyclones in the southern Pacific Ocean. Source: Chart created from the re-analysis of cyclone intensities by the authors.

208x76mm (72 x 72 DPI)

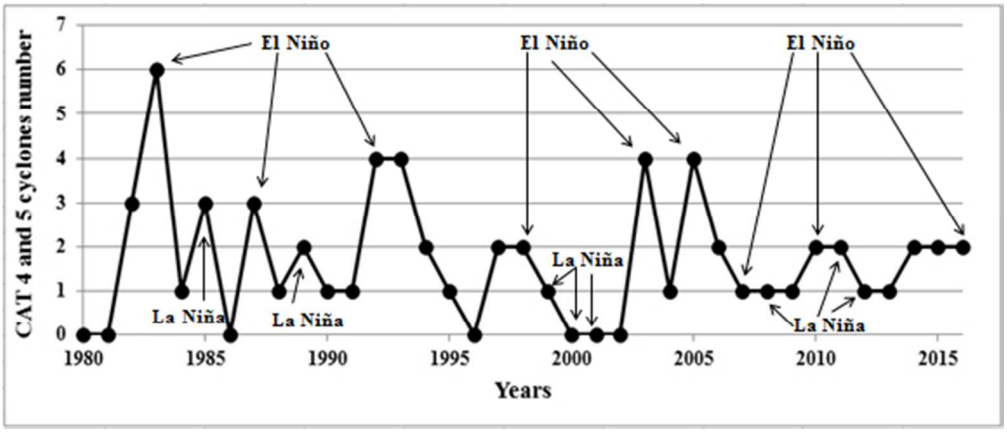


Figure 6. Annual number of extreme Cat 4-5 cyclones (1980-2016) and the El Niño, La Niña events. Source: Chart prepared using data from CPCM (2016) and the re-analysis of cyclone intensities by the authors.

203x86mm (72 x 72 DPI)

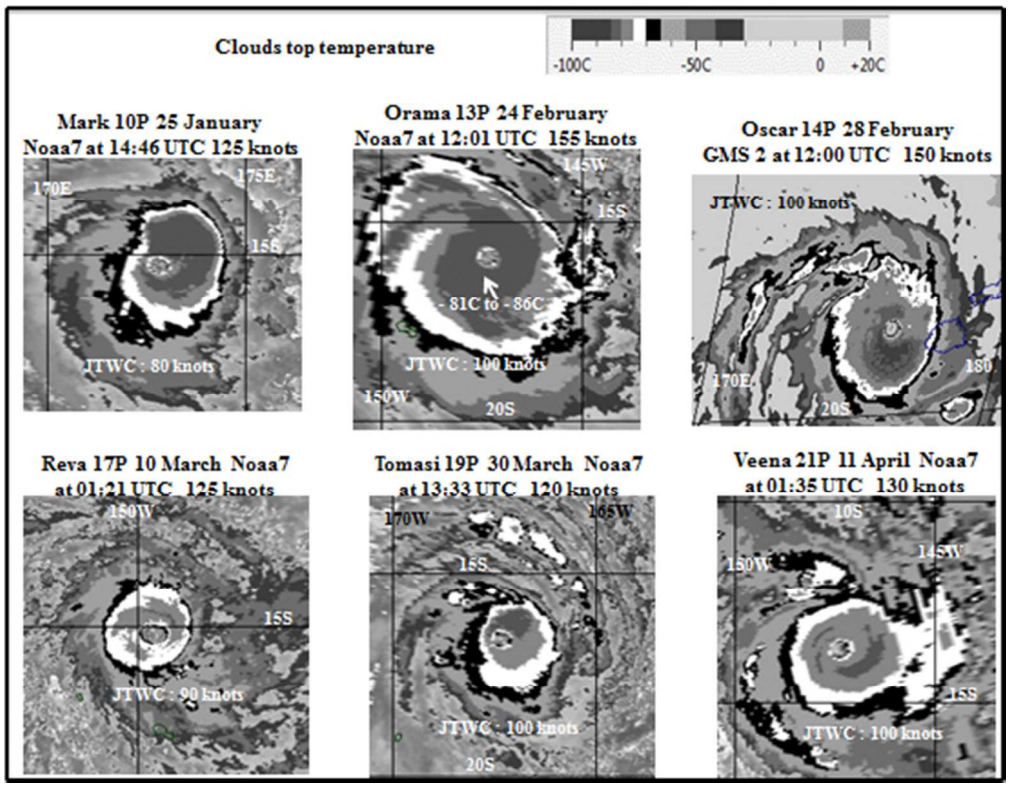


Figure 7. Satellite images (Basic Dvorak) of extreme cyclones during the 1983 season. Source: Images treated using raw data from NCDC.

194x150mm (72 x 72 DPI)

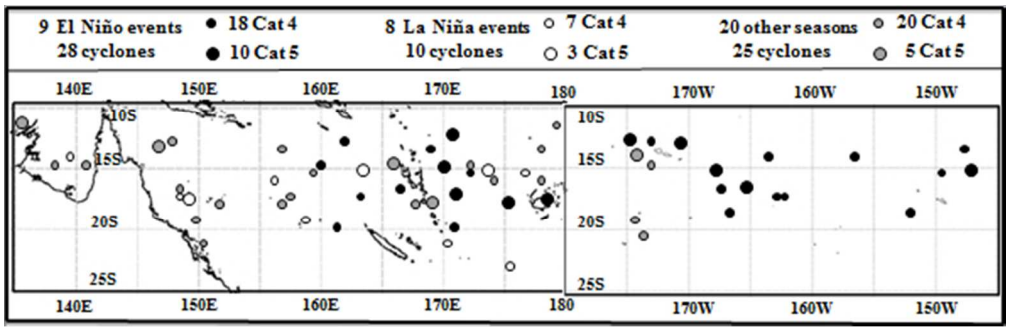


Figure 8. The location of the maximum intensity of extreme cyclones during El Niño, La Niña and the other seasons. Source: Chart prepared using data from CPMC (2016) and the re-analysis of cyclone intensities by the authors.

209x67mm (72 x 72 DPI)

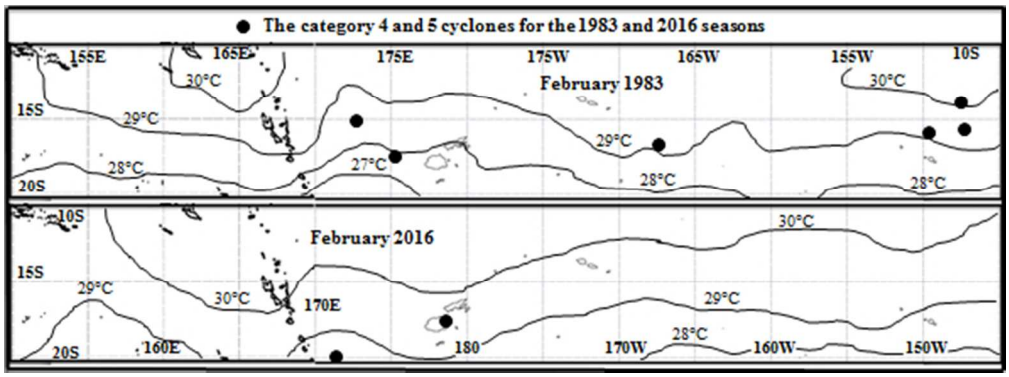


Figure 9. The location of the maximum intensity of extreme cyclones and the sea surface temperature during the two strongest El Niño events. Source: Chart prepared using data from NOAA/ESRL and from the re-analysis of cyclone intensities by the authors.

209x76mm (72 x 72 DPI)

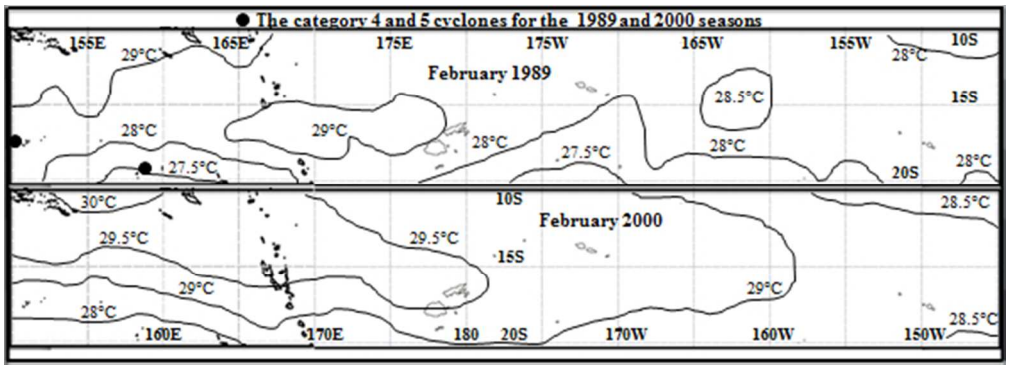


Figure 10. The location of the maximum intensity of extreme cyclones and the sea surface temperature during the two strongest La Niña events. Source: Chart prepared using data from NOAA/ESRL and from the re-analysis of cyclone intensities by the authors.

209x75mm (72 x 72 DPI)

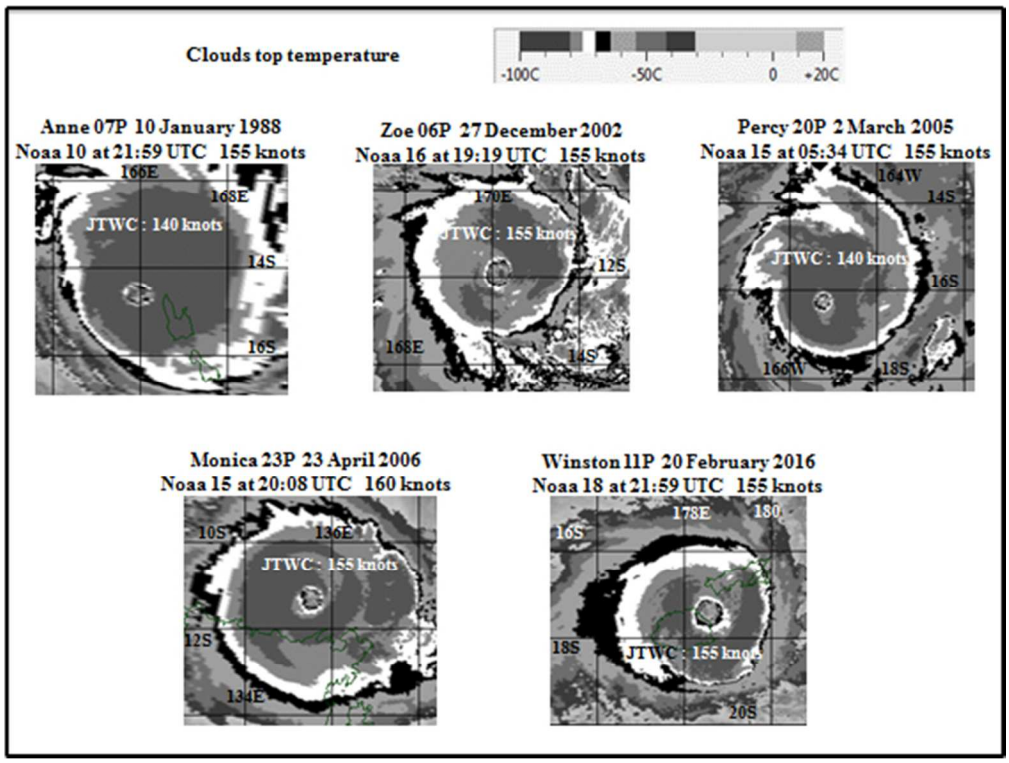


Figure 11. Satellite images (Basic Dvorak) of five of the seven strongest cyclones in the southern Pacific Ocean. Source: Images treated using raw data from NCDC.

199x150mm (72 x 72 DPI)

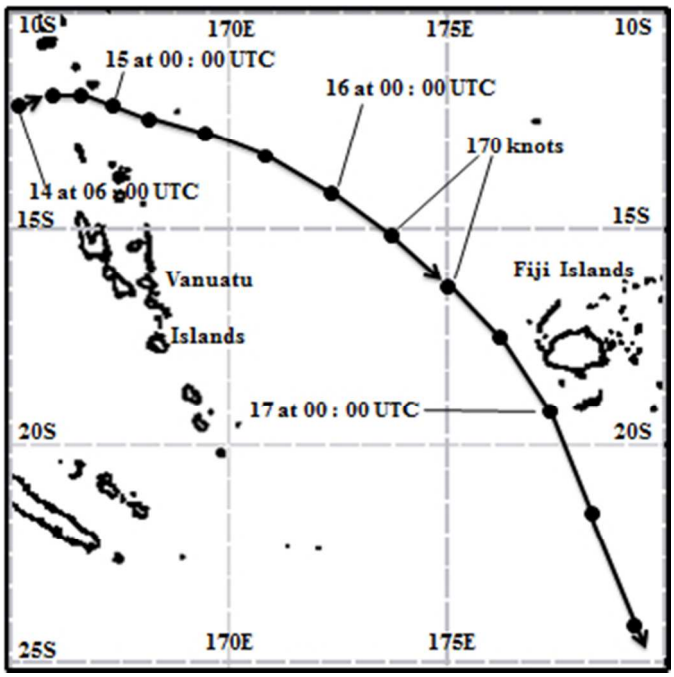


Figure 12. Trajectory of tropical cyclone Hina (March 1985). Source: Chart created from data of JTWC.

117x117mm (72 x 72 DPI)

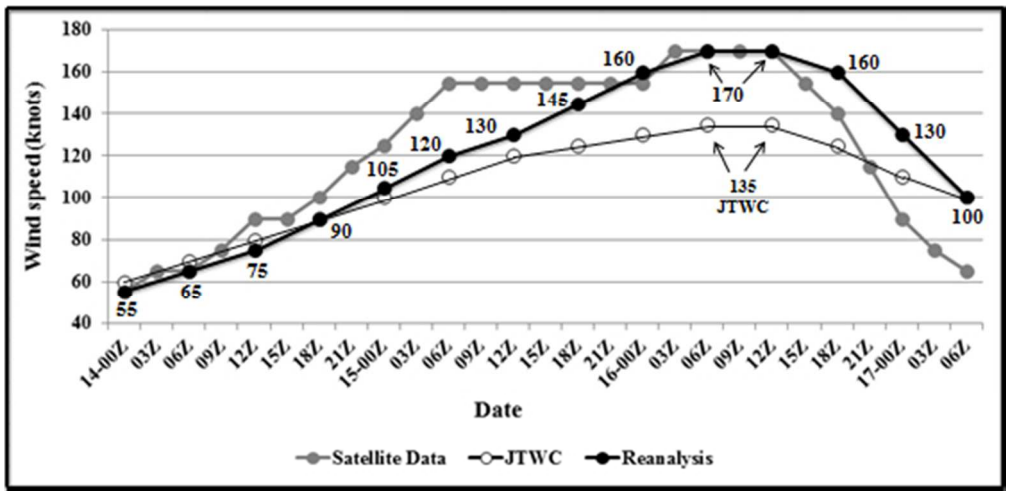


Figure 13. Estimation of the intensity of cyclone Hina using the Dvorak method. Source: Chart created from raw data provided by GMS, NOAA and JTWC.

197x95mm (72 x 72 DPI)

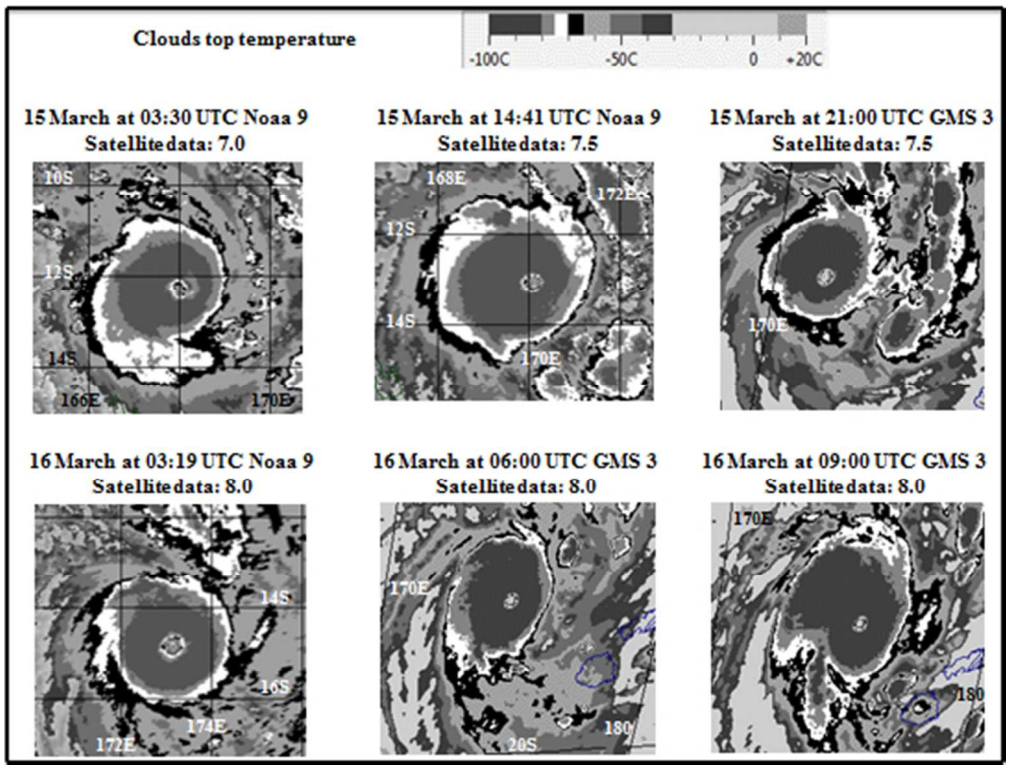


Figure 14. Satellite images (Basic Dvorak) of cyclone Hina. Source: Images treated using raw data from NCDC and JMA.

191x144mm (72 x 72 DPI)